



1 **An underappreciated cyclonic-like circulation drives high summer ozone in North China Plain**

2 Wenhao Qiao<sup>1,2</sup>, Xipeng Jin<sup>\*2</sup>, Xi Chen<sup>3</sup>, Ziyu Long<sup>2</sup>, Zhenjiang Yang<sup>2</sup>, Lei Chen<sup>2</sup>, Ke Li<sup>1,2</sup>, and  
3 Hong Liao<sup>1,2</sup>

4 <sup>1</sup>State Key Laboratory of Climate System Prediction and Risk Management, Joint International  
5 Research Laboratory of Climate and Environment Change (ILCEC), Collaborative Innovation Center  
6 of Atmospheric Environment and Equipment Technology, Nanjing University of Information Science  
7 & Technology, 210044 Nanjing, China

8 <sup>2</sup>School of Environmental Science and Engineering, Nanjing University of Information Science  
9 & Technology, 210044 Nanjing, China

10 <sup>3</sup>College of Geomatics, Zhejiang University of Water Resources and Electric Power, Hangzhou  
11 310018, China

12 *Correspondence to:* [xipengjin@nuist.edu.cn](mailto:xipengjin@nuist.edu.cn)

13 **Abstract.** China continues to experience severe ozone pollution, particularly over the North China  
14 Plain (NCP) during summer. Ozone pollution is generally considered to be associated with  
15 anticyclonic circulation. However, this study reveals that a previously underappreciated cyclonic-like  
16 circulation also plays a substantial role in ozone pollution over the NCP. Based on a systematic analysis  
17 of summertime observations from 2017 to 2022, we identify 209 ozone pollution days, 60 of which  
18 are associated with cyclonic-like circulation. Under cyclonic-like circulation, northwesterly winds  
19 prevail over the NCP. As the airflow crosses the Taihang Mountains, it undergoes adiabatic descent  
20 and induce foehn winds, leading to anomalous warming (+1.78 °C) and drying (−15 %) in the western  
21 NCP. Foehn-induced warming substantially enhances ozone photochemical production, resulting in  
22 severe ozone pollution over the western NCP, with MDA8 ozone concentrations exceeding 102.2 ppb.  
23 In addition, subsiding airflow transports ozone-rich air from the residual layer downward, leading to  
24 elevated nighttime ozone along the leeward foothills. Consequently, the impact of cyclonic-like  
25 circulation on ozone pollution is characterized by pronounced spatial heterogeneity, in contrast to the  
26 relatively uniform ozone enhancement over the NCP under anticyclonic circulation. More importantly,  
27 the frequency of cyclonic-like circulation exhibits an increasing trend during 1980-2024, suggesting  
28 its growing importance in modulating ozone pollution. We further demonstrate that emission control  
29 strategies should be tailored to different circulations. Under cyclonic-like circulation, local emission  
30 reductions within the NCP are most effective, whereas under anticyclonic circulation, reductions in  
31 the adjacent southeastern region yield greater mitigation benefits.



32 **Keywords:** Ozone pollution; cyclonic-like circulation; North China Plain; pollution control strategy

### 33 **1 Introduction**

34 China has been suffering from severe ozone pollution in recent years, despite the implementation of a  
35 series of stringent air pollution control measures (Liu et al., 2023a; Wang et al., 2022). Ozone has  
36 surpassed particulate matter to become the primary air pollutant in 339 cities in 2022 (MEE, 2023),  
37 posing serious threats to human health (Nuvolone et al., 2018; Fleming et al., 2018), ecosystem (Li et  
38 al., 2021a; Long et al., 2024), and climate (IPCC, 2023). The North China Plain (NCP), as the most  
39 severely ozone pollution area in China, frequently experiences ozone concentrations exceeding 160  
40  $\mu\text{g m}^{-3}$ , especially in summer (Lu et al., 2018; Wang et al., 2020; Wang et al., 2022). For example, in  
41 June 2024, the average ozone concentration in Beijing-Tianjin-Hebei and surrounding areas even  
42 reached 220  $\mu\text{g m}^{-3}$ , far exceeding the national air quality standards (MEE, 2024). Elucidating the  
43 dominant factors contributing to ozone pollution in the NCP is essential for advancing the  
44 understanding of its occurrence mechanisms and developing effective control strategies.

45 Ozone is a secondary air pollutant formed through photochemical reactions of volatile organic  
46 compounds (VOCs) and nitrogen oxides ( $\text{NO}_x$ ), and its levels are jointly controlled by precursor  
47 emissions, chemical processes, and meteorological conditions. Emissions of ozone precursors and their  
48 photochemical formation have been extensively investigated (Liu et al., 2023b; Wang et al., 2022; Xie  
49 et al., 2023). VOCs and  $\text{NO}_x$  are emitted primarily from fuel combustion and industrial activities, with  
50 additional contributions from biogenic processes and agricultural soil emissions, respectively (Li et al.,  
51 2022; Weng et al., 2020). The photochemical production of ozone is highly nonlinear, which is  
52 generally considered to be VOC-limited in urban areas and  $\text{NO}_x$ -limited in rural regions (Li et al., 2024;  
53 Zhang et al., 2025). With the substantial reductions in  $\text{NO}_x$  emissions in recent years, some urban areas  
54 have gradually shifted toward  $\text{NO}_x$ -limited or transitional regimes (Wang et al., 2025; Xue et al., 2026).  
55 Beyond emissions and chemical processes, meteorological conditions also play a critical role in ozone  
56 pollution, which not only influence the rates of photochemical reactions and the magnitude of  
57 emissions but also govern the transport and dispersion of pollutants.

58 Previous studies have explored the role of meteorological conditions in ozone pollution from two  
59 perspectives: individual meteorological factors and large-scale circulation patterns. High temperatures  
60 have been shown to enhance both biogenic and anthropogenic VOC emissions (Tarvainen et al., 2005;



61 Qin et al., 2025) and to promote photochemical reactions (Lee et al., 2014; Fu et al., 2015), thereby  
62 exacerbating ozone pollution. Strong solar radiation favors the photochemical formation of ozone  
63 (Chen et al., 2024; Jiang et al., 2025). In contrast, increased relative humidity can lead to a decrease in  
64 ozone concentrations in the lower troposphere (Kalabokas et al., 2015). Wind fields also play a critical  
65 role by transporting ozone and its precursors (Lu et al., 2019; Qu et al., 2024), while clouds can  
66 suppress ozone levels through liquid-phase chemistry and photochemistry, which reduces atmospheric  
67 oxidative capacity via oxidant removal (Lelieveld et al., 1990).

68 Large-scale circulation patterns serve as the synoptic background driving the evolution of ozone  
69 pollution. Previous studies have generally reported that high-ozone episodes are primarily associated  
70 with anticyclonic systems, based on both synoptic classification and composite analyses (Hart et al.,  
71 2006; Hegarty et al., 2007; Gong et al., 2019; Dong et al., 2020). For example, Pope et al. (2016)  
72 applied Lamb's (1972) approach to classify UK summer circulation patterns into three types, showing  
73 that ozone pollution is more severe under anticyclonic weather type. Dong et al. (2020) classified the  
74 circulation patterns in the NCP into four types using the T-mode Principal Component Analysis (T-  
75 PCA) method, and demonstrated that anticyclonic circulation favors ozone pollution. Similar findings  
76 are also reported by Gong et al. (2019), who, based on composite analyses, found that the ozone  
77 pollution in the NCP is typically associated with anticyclonic circulation. Therefore, it is widely  
78 recognized that ozone pollution over the NCP predominantly occurs under anticyclonic conditions,  
79 which are typically accompanied by high temperatures, low humidity, and southerly transport,  
80 facilitating ozone chemical formation and accumulation.

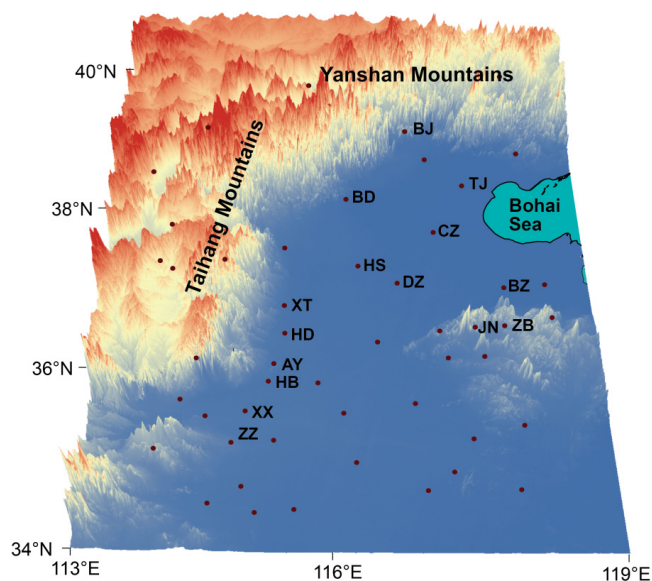
81 In this study, we show an underappreciated cyclonic-like circulation that drives high ozone levels in  
82 the NCP, based on a systematic analysis of summertime observations during 2017–2022. The  
83 characteristics of this cyclonic-like circulation and its impacts on ozone pollution are elucidated. In  
84 addition, the long-term trend of the cyclonic-like circulation and the implications for regional emission  
85 control are investigated. The remainder of this paper is organized as follows. Section 2 describes the  
86 data and methodology. Section 3 presents the results and discussion. Section 4 summarizes the main  
87 findings.

## 88 **2 Data and methodology**

### 89 **2.1 Research area and observational data**



90 The NCP is one of the largest plains in China, spanning 34–41°N and 113–119°E. It encompasses the  
91 Beijing–Tianjin–Hebei (BTH) metropolitan region and surrounding areas, with dense population and  
92 industry. This region consists of a vast flat plain surrounded by the Taihang Mountains to the west, the  
93 Yanshan Mountains to the north, and the Bohai Sea to the east (**Fig. 1**). This unique topographic  
94 configuration, with mountains on two sides and an open boundary toward the ocean, plays a crucial  
95 role in modulating atmospheric circulation and air pollution evolution.



96  
97 **Figure 1.** Topography of the research area and locations of ozone concentration observation stations

98 Hourly near-surface ozone concentration data over the NCP were obtained from China's National Air  
99 Quality Monitoring Network (URL: [datacenter.mee.gov.cn/websjzx/queryIndex.vm](http://datacenter.mee.gov.cn/websjzx/queryIndex.vm)), which was  
100 established by Ministry of Ecology and Environment (MEE) in 2012. O<sub>3</sub> concentrations were reported  
101 by the MEE in micrograms per cubic meter ( $\mu\text{g m}^{-3}$ ) under standard conditions (273 K, 1013 hPa)  
102 until 31 August 2018; this reference state was revised to 298 K and 1013 hPa for gaseous species since  
103 1 September 2018. In this study, ozone concentrations were consistently converted to parts per billion  
104 (ppb) and observations from 39 urban stations across the NCP were selected for analysis (**Fig. 1**).

105 The maximum daily 8-h average (MDA8) O<sub>3</sub> concentration was calculated following the Ambient Air  
106 Quality Standards (GB3095-2012). To ensure data quality, the 8-h sliding average must contain more  
107 than 6 h of valid observations, and the number of valid MDA8 O<sub>3</sub> days per month must be greater than



108 15 days at each site. The ozone pollution day was defined as a day when the regional mean MDA8 O<sub>3</sub>  
109 concentration over the NCP exceeded 82 ppb. A total of 209 ozone pollution days were identified  
110 during the summers (June–August) of 2017–2022.

## 111 2.2 GEOS-Chem model

112 The GEOS-Chem (Goddard Earth Observing System Chemical Transport Model) is a global three-  
113 dimensional atmospheric chemistry model. In this study, GEOS-Chem v13.3.3 ([https://geos-  
114 chem.seas.harvard.edu/](https://geos-chem.seas.harvard.edu/)) was employed to simulate surface ozone over China during the summer  
115 months from 2017 to 2022. The model includes fully coupled tropospheric and stratospheric ozone-  
116 NO<sub>x</sub>-VOCs-HO<sub>x</sub>-aerosol chemical regimes (Dang et al., 2021). The wet deposition scheme was  
117 adopted from Liu et al. (2001) and the dry deposition scheme was adopted from the standard drag  
118 sequence model of Wesely (2007). Vertical mixing within the planetary boundary layer was modelled  
119 using a non-local mixing scheme. The simulations were performed in a nested domain (11°–55°S, 60-  
120 150°E) with a horizontal resolution of 0.5° latitude by 0.625° longitude and 47 vertical layers. The  
121 boundary conditions were provided by the GEOS-Chem global simulation with a horizontal resolution  
122 of 2° latitude by 2.5° longitude.

123 The GEOS-Chem simulations were driven by MERRA-2 reanalysis data (Modern Era Retrospective  
124 Analysis for Research and Application, Version 2). The anthropogenic source emissions were obtained  
125 from the MEIC (Multi-resolution Emission Inventory model for Climate and air pollution research)  
126 inventory. In terms of natural emissions, biogenic volatile organic compounds (VOCs), soils, and flash  
127 NO<sub>x</sub> were calculated online in the model following the methodology of Li et al. (2021b). The LIONZ  
128 programme was used for stratospheric ozone chemistry (McLinden et al., 2000).

129 In this study, we conducted simulations for June of 2017–2022 to investigate the impact of cyclonic-  
130 like circulations on ozone pollution, in which anthropogenic emissions were fixed at 2017 levels to  
131 eliminate the influence of interannual variability of emission. In addition, emission reduction  
132 experiments were performed over three regions: the NCP, its adjacent northwestern region (NW,  
133 34°N–42°N; 107°E–112.5°E, **Fig. S1**), and its adjacent southeastern region (SE, 28°N–33.5°N; 113°E–  
134 122°E, **Fig. S1**). In each region, VOC and NO<sub>x</sub> emissions were synergistically reduced by 10%, 30%,  
135 and 50%, respectively, to evaluate which region's emission control is most effective in mitigating  
136 ozone pollution over the NCP under different circulation patterns.



137 **2.3 Identification of cyclonic-like circulation**

138 Under large-scale cyclonic-like circulation, northwesterly winds typically prevail over the NCP, as  
139 reported by previous studies (Gu et al., 2023; Yan et al., 2024; Li et al., 2025). Therefore, northwesterly  
140 winds can serve as an indicator of cyclonic-like circulation. In this study, we follow Chen and Lu  
141 (2016), in which large-scale cyclonic-like circulation is diagnosed based on the anomalous  
142 northwesterly winds at 850 hPa along a transect from 42° N, 108° E to 38° N, 112° E. Considering  
143 that the selection of transect may affect the identification of circulation patterns, seven transects were  
144 designed and evaluated in this study (**Fig. S1**). Validation against manual expert identification  
145 indicates that transect 3 (from 40°N, 111.25°E to 37.5°N, 114.375°E) produces the most reliable results,  
146 outperforming the transect configuration used in Chen and Lu (2016). Accordingly, we adopted the  
147 850 hPa northwesterly winds averaged along the transect from 40° N, 111.25° E to 37.5° N, 114.375°  
148 E as the cyclonic-like circulation index.

149 Among the 209 ozone pollution days during the summers of 2017-2022, 60 cyclonic-like circulation  
150 days were identified, accounting for 29% of all pollution days. This finding suggests that nearly one-  
151 third of ozone pollution are associated with cyclonic-like circulation, rather than being exclusively  
152 controlled by anticyclonic circulation, underscoring the necessity of investigating the influence of  
153 cyclonic-like circulation on ozone pollution.

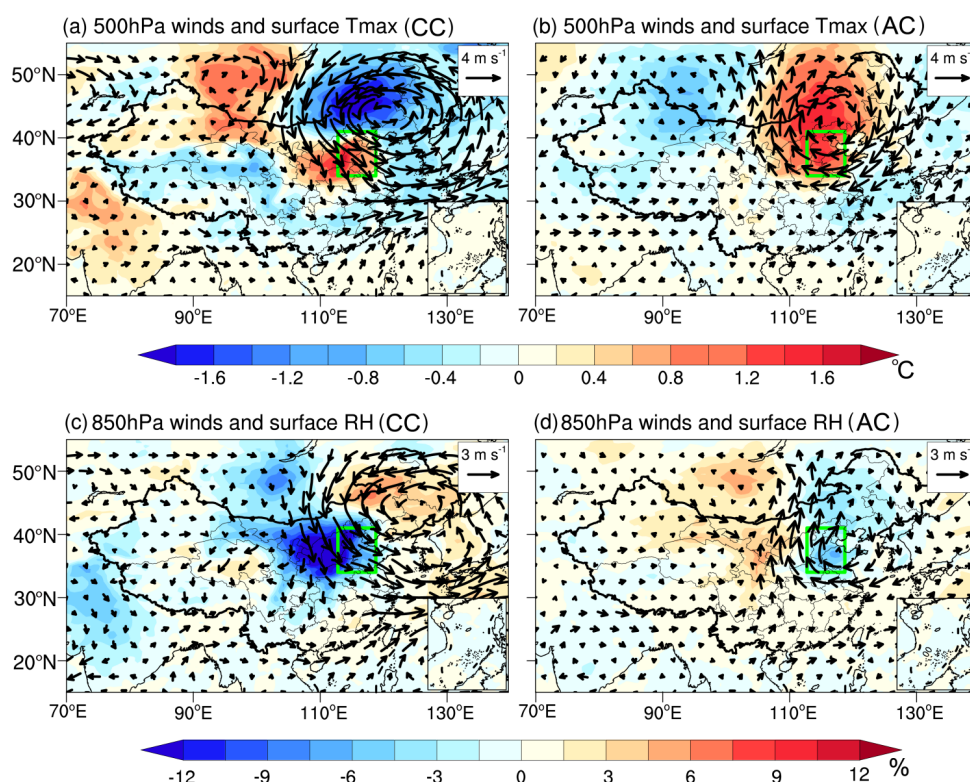
154 **3 Results and discussion**

155 **3.1 Characteristics of the cyclonic-like circulation**

156 The synoptic characteristics of cyclonic-like circulation associated with ozone pollution during the  
157 summers of 2017 to 2022 are revealed (cyclonic-like and anticyclonic circulations in this study refer  
158 specifically to conditions during ozone pollution days). **Figure 2a** and **2d** present the wind fields at  
159 500 hPa and 850 hPa, as well as the surface temperature and relative humidity under cyclonic-like  
160 circulation. It can be observed that a counterclockwise circulation is evident at both 500 and 850 hPa  
161 across North China and Northeast China, indicating a well-developed cyclonic system. The NCP is  
162 located within the northwesterly wind quadrant of this circulation, with surface temperatures and  
163 relative humidity displaying positive and negative anomalies, respectively (regional means of +0.68 °C  
164 and -8.2 %). The most pronounced warming and drying signals occur in the western NCP and  
165 maximum anomalies reach +1.78 °C and -15 %, respectively. The above features are different from



166 the well-known anticyclonic circulation accompanying ozone pollution (**Fig. 2b and 2e**), which is  
 167 characterized by anomalous southerly winds, widespread elevated surface temperature, and decreased  
 168 humidity over the NCP (regional means of +1.1 °C and -3.5 %), as widely reported in previous ozone  
 169 studies (Gong et al., 2019; Dong et al., 2020). Although both circulation types induce surface warming  
 170 and drying, the effects of cyclonic-like circulation are more spatially concentrated and pronounced in  
 171 the western NCP.

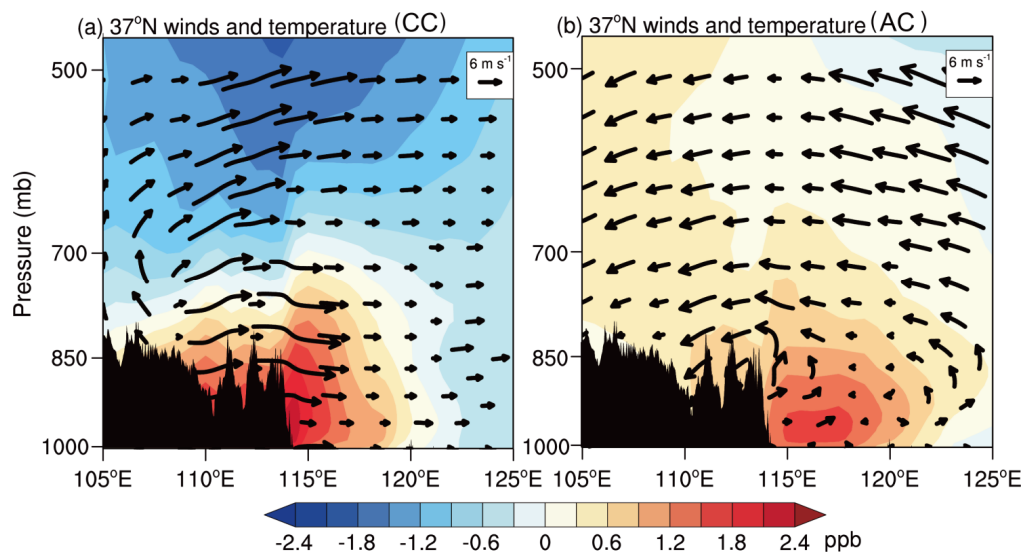


172  
 173 **Figure 2.** Spatial patterns of cyclonic-like circulation (CC, left) and anticyclonic circulation (AC, right)  
 174 associated with ozone pollution days during the summers of 2017-2022. (a, b) Anomalous 500 hPa  
 175 winds (vectors) and surface maximum temperature (filled colors) under CC and AC conditions. (c, d)  
 176 Anomalous 850 hPa winds (vectors) and surface relative humidity (filled colors) under CC and AC  
 177 conditions. Anomalies are calculated by subtracting the corresponding multi-year mean for June, July,  
 178 and August, respectively. The green rectangles denote the NCP.

179 To investigate the distinct warming characteristics induced by cyclonic-like circulation and their  
 180 differences from those under anticyclonic circulation, vertical cross-sections of temperature and wind



181 vector anomalies along 37°N from 105°E to 125°E are presented in **Fig. 3**. Under cyclonic-like  
 182 circulation, horizontal westerly winds prevail along the cross-section. As the flow passes over the  
 183 Taihang Mountains, descending motion occurs on the leeward side, where positive temperature  
 184 anomalies present (**Fig. 3a**). The most pronounced warming is concentrated in the area adjacent to the  
 185 mountains, with peak values exceeding 2.5 °C, while the positive temperature anomalies decrease  
 186 significantly and even turn negative with increasing distance eastward from the mountains. This  
 187 localized, subsidence-accompanied warming, points to the foehn phenomenon, which is induced by  
 188 adiabatic heating and drying of airflow descending after crossing the mountains (M. Matějka, et al.,  
 189 2025). Taken together, cyclonic-like circulation makes northwesterlies prevail over the mountains,  
 190 creating conditions conducive to the foehn effect and resulting in localized warming and drying over  
 191 the western NCP. This contrasts with the widespread and uniform positive temperature anomalies  
 192 under anticyclonic circulation, which extend eastward across the entire NCP to 120°E (**Fig. 3b**).



193

194 **Figure 3.** Vertical cross-sections of anomalous temperature and wind vectors along 37°N from 105°E  
 195 to 125°E under (a) cyclonic-like circulation and (b) anticyclonic circulation. The vertical wind  
 196 component is multiplied by a factor of 300 when plotting the wind vector fields. Anomalies are  
 197 calculated by subtracting the corresponding multi-year mean for June, July, and August, respectively.

198 We further elucidate the monthly variability of cyclonic-like circulation and its induced warming over  
 199 the western NCP. Cyclonic-like circulation occurs most frequently in June (38 days), accounting for

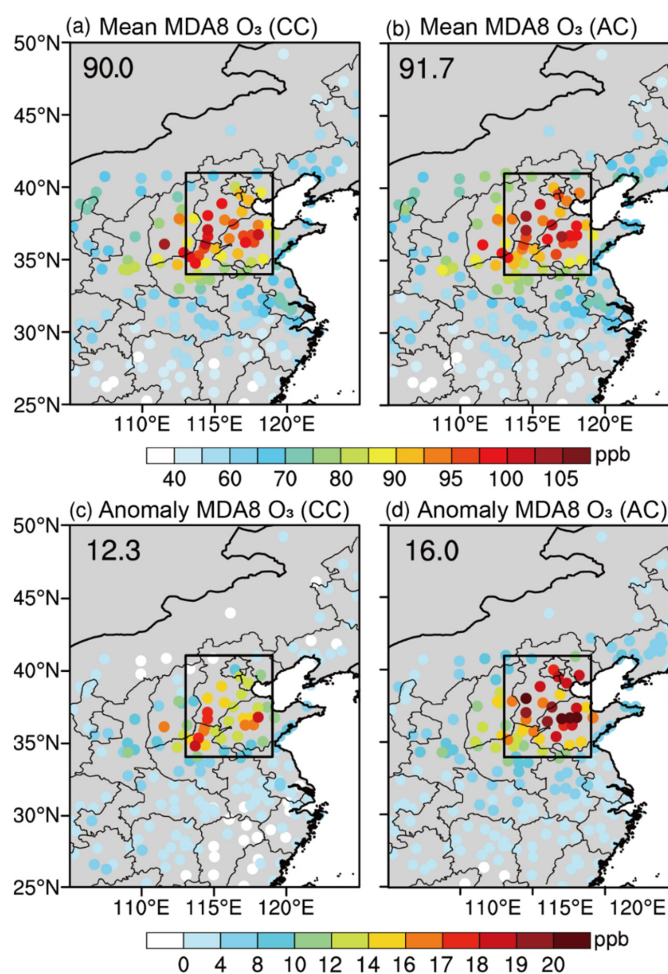


200 63% of all cyclonic days (60 days) during summer, which leads to a significantly greater temperature  
201 increase over the western plain compared with anticyclonic circulation (**Fig. S2a**). In July and August,  
202 cyclonic-like circulation occurred on 16 and 6 days, respectively, with temperatures comparable to or  
203 slightly lower than those under anticyclonic circulation (**Fig. S2b-c**). It can be concluded that June is  
204 the month during which cyclonic-like circulation exerts the most substantial warming effect.

205 In summary, cyclonic-like circulation is characterized by prevailing northwesterly winds over the NCP,  
206 which favor the development of foehn effects, leading to pronounced localized warming and drying  
207 over the western NCP, particularly concentrated on the leeward side of the Taihang Mountains. This  
208 pattern contrasts with the widespread and uniform warming under anticyclonic circulation and is most  
209 pronounced in June. Based on these identified characteristics of cyclonic-like circulation, its impacts  
210 on ozone pollution are further investigated in the following section.

### 211 **3.2 Impacts of the cyclonic-like circulation on ozone pollution**

212 **Figure 4** shows the spatial distribution of mean ozone concentrations under cyclonic-like circulation  
213 and their anomalies relative to the summer mean over 2017-2022, as well as the corresponding patterns  
214 under anticyclonic circulation for comparison. It can be found that under cyclonic-like circulation,  
215 ozone pollution is spatially heterogeneous over the NCP, with the most severe pollution mainly  
216 occurring in the western area along the Taihang Mountains, where concentrations exceed 102.2 ppb,  
217 while other regions experience relatively weaker pollution, yielding a regional mean of 90.0 ppb (**Fig.**  
218 **4a**). In contrast, under anticyclonic circulation, ozone pollution is more uniformly distributed, with a  
219 regional mean concentration of 91.7 ppb (**Fig. 4b**). The anomaly fields more clearly present the spatial  
220 heterogeneity of ozone pollution (**Fig. 4c**). Under cyclonic-like circulation, markedly enhanced  
221 positive ozone anomalies are primarily concentrated on the leeward foothills of the Taihang Mountains,  
222 reaching as high as +19.3 ppb, whereas increases at other stations are relatively modest. This spatial  
223 heterogeneity is in stark contrast to the widespread ozone enhancement under anticyclonic circulation  
224 over the NCP (**Fig. 4d**), which corresponds well to the spatial distribution of anomalous warming (**Fig.**  
225 **2 and Fig. S3**).



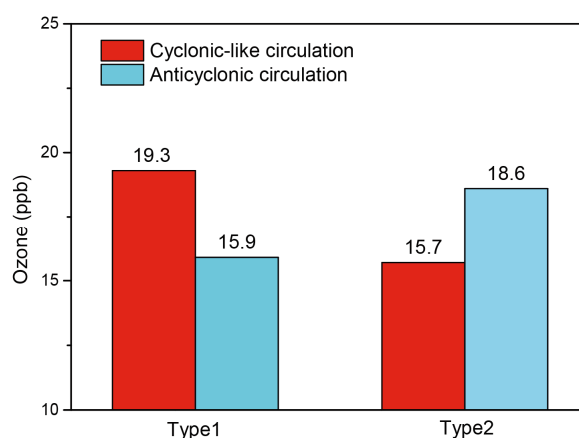
226

227 **Figure 4.** Spatial distribution of (a, b) mean MDA8 ozone concentrations under cyclonic-like and  
 228 anticyclonic circulations and (c, d) their anomalies relative to the average over the summers of 2017-  
 229 2022. The black rectangles denote the NCP.

230 The above analysis indicates that, although the regionally averaged ozone pollution levels are  
 231 comparable under the two circulations, their spatial patterns differ markedly. According to the  
 232 distribution characteristics of ozone pollution, the stations are classified into two categories: those  
 233 located along the leeward foothills of the Taihang Mountains in the western NCP (Type 1), and those  
 234 situated over the central and eastern plains (Type 2, the locations of the two types of stations are shown  
 235 in **Fig. 1**). This classification enables a more detailed investigation of the impacts of cyclonic-like  
 236 circulation on ozone pollution, as well as its differences from anticyclonic circulation. As shown in  
 237 **Fig. 5**, ozone concentration at Type 1 stations increases by 19.3 ppb under cyclonic-like circulation



238 relative to the summer mean, which is larger than the increase under anticyclonic circulation (15.9  
239 ppb). In contrast, at Type 2 stations, the ozone increases under cyclonic-like circulation (15.7 ppb) is  
240 smaller than that under anticyclonic circulation (18.6 ppb). This suggests that cyclonic-like circulation  
241 exerts a stronger influence on ozone enhancement over the western NCP, whereas its effect over the  
242 central and eastern plain is weaker than that of anticyclonic circulation.



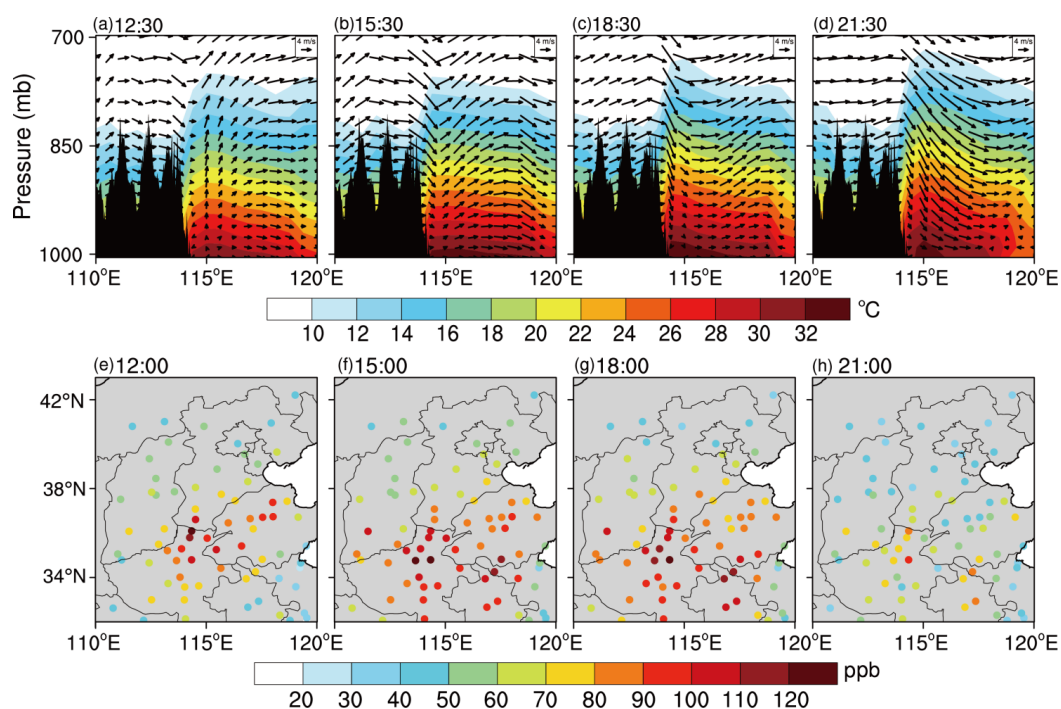
243

244 **Figure 5.** Ozone concentration anomalies at two types of stations under cyclonic-like and anticyclonic  
245 circulations relative to the summer mean during 2017–2022. Type 1 stations are located along the  
246 leeward foothills of the Taihang Mountains in the western NCP, including XT, HD, AY, HB, XX and  
247 ZZ. Type 2 stations are situated over the central and eastern plains, including BJ, BD, TJ, CZ, HS, DZ,  
248 BZ, JN and ZB. The locations of these stations are shown in Fig. 1.

249 A typical case provides a more comprehensive understanding of the impact of cyclonic-like circulation  
250 on ozone pollution. On 5 June 2022, the NCP was under the control of a cyclonic-like circulation,  
251 characterized by prevailing northwesterly winds (**Fig. S4**), during which the MDA8 ozone  
252 concentration over the western NCP reached up to 103.2 ppb. **Figure 6** illustrates the vertical cross-  
253 sections of temperature and wind vectors along 37°N from 110°E to 120°E and the spatial distribution  
254 of surface ozone concentration over the NCP. About 12:00 LT, northwesterly winds begin to develop  
255 over the NCP, inducing weak descending motion on the leeward side of the Taihang Mountains (**Fig.**  
256 **6a**). The adiabatic descent of airflow leads to enhanced warming over the western plains, with a greater  
257 vertical extent of influence, as evidenced by isotherms tilting downward from the western part near  
258 the mountains toward the more distant eastern plains (**Fig. 6a**). The largely elevated temperatures at  
259 the foothills enhance ozone photochemical production, resulting in significantly higher ozone



260 concentrations at western stations compared with other stations across the NCP (**Fig. 6e**). By 15:00  
 261 and 18:00 LT, the westerly winds, the downslope flow after crossing the mountains, and the associated  
 262 warming become more pronounced (**Fig. 6b-c**), making ozone concentrations at foothill stations  
 263 remain at elevated levels. Meanwhile, ozone concentrations at downwind stations also increase (**Fig.**  
 264 **6f-g**), which is partly attributable to northwesterly transport, in addition to the local chemical formation  
 265 (**Fig. S4**). At 21:00 LT, the subsiding airflow over the Taihang mountains remains evident (**Fig. 6d**),  
 266 which facilitate the downward transport of ozone-rich air from the residual layer aloft to the surface.  
 267 This process sustains relatively higher ozone concentrations at foothill stations compared with other  
 268 stations, where ozone is effectively depleted by NO titration at night (**Fig. 6h**).



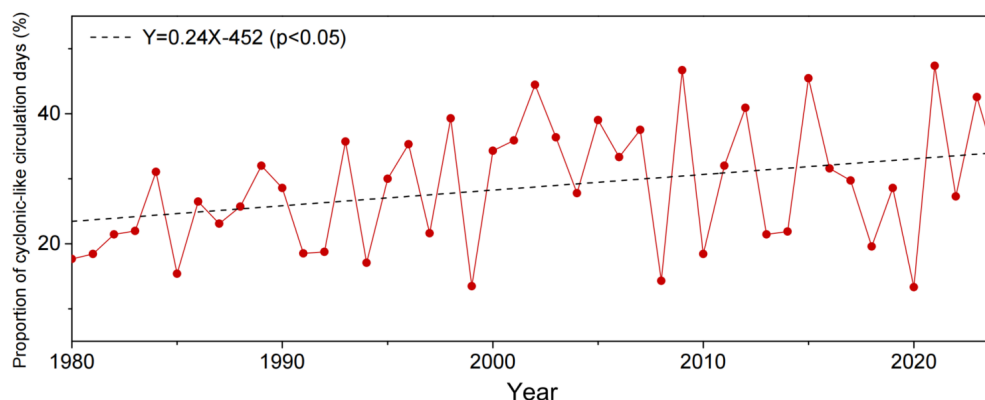
269  
 270 **Figure 6.** Vertical cross-sections of temperature and wind vectors along 37° N from 110°E to 120°E  
 271 (upper panel) and spatial pattern of surface ozone concentration (lower panel) on 5 June 2022 at (a, e)  
 272 12:30 and 12:00, (b, f) 15:30 and 15:00, (c, g) 18:30 and 18:00, (d, h) 21:30 and 21:00. The vertical  
 273 cross-sections of temperature and wind vectors are obtained from MERRA-2 data, while the surface  
 274 ozone concentrations are from hourly observations, with a 30-minute time offset between the two  
 275 datasets.



276 Both the composite analysis and the case study consistently demonstrate that cyclonic-like circulation  
277 plays a crucial role in ozone pollution over the NCP, exhibiting pronounced spatial heterogeneity with  
278 particularly strong impacts over the western plain. This is primarily attributed to foehn-induced  
279 warming as northwesterly flow crosses the Taihang Mountains, which enhances ozone photochemical  
280 production. In addition, descending motion associated with foehn transports ozone-rich air from the  
281 residual layer downward, resulting in higher nighttime surface ozone concentrations than in other  
282 regions. Further, prevailing northwesterly winds can transport ozone pollution to downwind areas,  
283 contributing to a moderate increase in ozone concentrations across other parts of the NCP.

### 284 3.3 Long-term trends and implications for emission reduction

285 Given the important role of cyclonic-like circulation in ozone pollution, we further investigate its long-  
286 term trend from 1980 to 2024. As shown in **Fig. 7**, the frequency of cyclonic-like circulation on days  
287 with temperatures exceeding 32 °C in the NCP exhibits a significant increasing trend of 0.24% yr<sup>-1</sup>  
288 ( $p < 0.05$ ) during the past 45 years. The focus on days with temperatures above 32 °C (the average  
289 temperature of ozone pollution days) is motivated by the lack of long-term ozone concentration  
290 observations. Nevertheless, the strong association between high temperatures and ozone pollution  
291 allows temperature to serve as a reasonable proxy for assessing long-term changes (Li et al., 2024;  
292 Xing et al., 2026; Xu et al., 2025). This upward trend indicates that cyclonic-like circulation is  
293 becoming an increasingly important driver of ozone pollution in the NCP, highlighting the urgency of  
294 developing ozone pollution control strategies tailored to this circulation pattern.

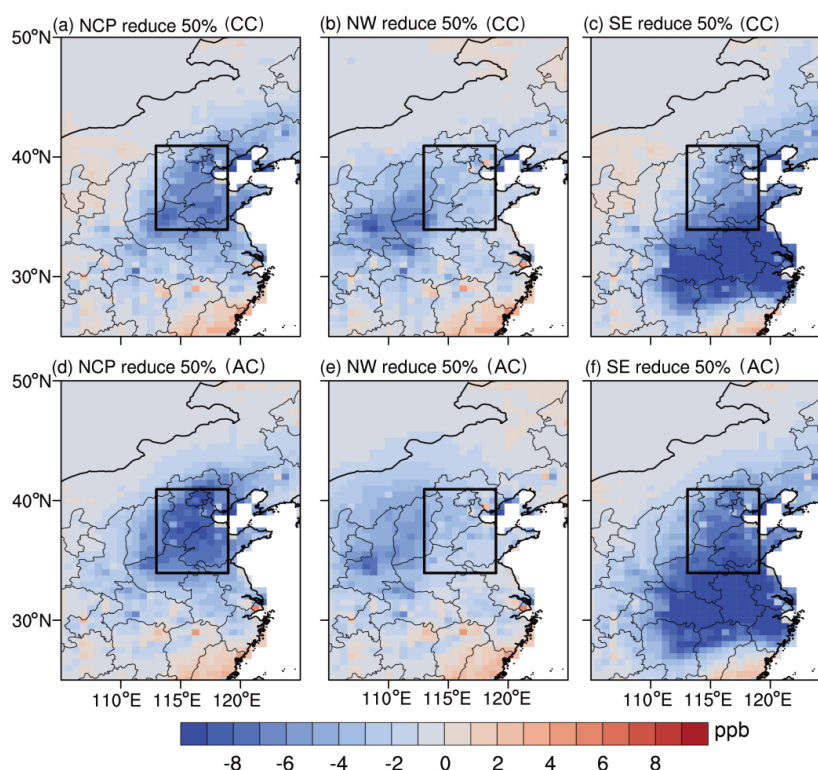


295  
296 **Figure 7.** Long-term trends of the proportion of cyclonic-like circulation on days with temperatures  
297 exceeding 32 °C in the NCP in summer from 1980 to 2024. The dash line indicates the linear fitting  
298 trend, with a slope of 0.24% yr<sup>-1</sup>.



299 To investigate which region's emission control is most effective in mitigating ozone pollution over the  
300 NCP under cyclonic-like and anticyclonic circulations, respectively, we conduct a series of sensitivity  
301 experiments using the GEOS-Chem model with precursor emission reductions within the NCP as well  
302 as in the adjacent regions to its northwest (NW) and southeast (SE) (**Fig. S1**). The model performance  
303 is first assessed through a comparison between the base simulation and observations. The simulated  
304 ozone concentrations show good agreement with observations, with correlation coefficients of 0.87  
305 and 0.91 under cyclonic-like and anticyclonic circulations, respectively (**Fig. S5**). More importantly,  
306 the model captures the distinct spatial patterns of ozone pollution, including the pronounced  
307 heterogeneity with high concentrations over the western NCP under cyclonic-like circulation, and the  
308 comparatively uniform distribution under anticyclonic circulation. These evaluations suggest that the  
309 model can reliably simulate ozone pollution, providing a solid basis for further analysis of the emission  
310 reduction simulation experiments.

311 **Figure 8** illustrates the reductions in ozone concentrations resulting from 50% decreases in both NO<sub>x</sub>  
312 and VOCs emissions over the NCP, NW, and SE regions, respectively. It can be observed that under  
313 the cyclonic-like circulation, emission reductions within the NCP itself yield the largest decrease in  
314 ozone concentrations (approximately 5.6 ppb, **Fig. 8a**), while reductions in the NW and SE regions  
315 result in a decrease of about 2.8 and 4.8 ppb of ozone concentration over the NCP, respectively (**Fig.**  
316 **8b-c**). This may be attributed to that ozone pollution under this circulation pattern is mainly driven by  
317 enhanced local photochemical formation induced by anomalous warming associated with foehn effect.  
318 In contrast, under anticyclonic circulation, the mitigation of ozone pollution over the NCP is most  
319 strongly influenced by emission reductions in the SE region, leading to a decrease of 7.2 ppb (**Fig. 8f**),  
320 because ozone pollution is usually accompanied by southerly transport. Emission reductions within  
321 the NCP also result in a 6.9 ppb decrease in ozone concentrations, underscoring the necessity of  
322 regional cooperative emission control under anticyclonic circulation. Simultaneous reductions of NO<sub>x</sub>  
323 and VOCs by 10% and 30% also exhibit similar patterns of ozone concentration decreases (**Fig. S6-**  
324 **S8**). These results imply that emission control strategies should be tailored to different circulation  
325 patterns. Under cyclonic-like circulation, local emission reductions are the most effective in the NCP,  
326 whereas under anticyclonic circulation, coordinated emission reductions in both the NCP and the SE  
327 region are required to achieve more effective ozone mitigation.



328

329 **Figure 8.** Response of MDA8 ozone concentration to 50% reductions in both NO<sub>x</sub> and VOCs  
 330 emissions in the (a, d) NCP, (b, e) NW, and (c, f) SE regions under cyclonic-like circulation (upper  
 331 panel) and anticyclonic circulation (lower panel). The black rectangles denote the NCP. The NW and  
 332 SE regions are indicated in Fig. S1.

### 333 4 Conclusions

334 This study reveals a previously underrecognized cyclonic-like circulation pattern that contributes to  
 335 ozone pollution over the NCP, based on a systematic analysis of summer ozone pollution during 2017-  
 336 2022. The distinctive meteorological patterns associated with cyclonic-like circulation are analyzed.  
 337 The spatial heterogeneity of their impacts on ozone pollution and the underlying mechanisms are  
 338 further elucidated. Additionally, the long-term trend of cyclonic-like circulation and the effectiveness  
 339 of emission control strategies under different circulation patterns are also investigated.

340 During the summers of 2017–2022, a total of 209 ozone pollution days are identified, of which 60  
 341 occur under cyclonic-like circulation, while the remaining days are dominated by anticyclonic  
 342 circulation. Under cyclonic-like circulation, the NCP is dominated by northwesterly airflow. As the



343 air mass crosses the southwest–northeast-oriented Taihang Mountains, it undergoes adiabatic descent  
344 and warming, inducing foehn winds. This process leads to localized and pronounced warming and  
345 drying over the western NCP, particularly along the leeward foothills of the Taihang Mountains. This  
346 contrasts with the spatially uniform warming and drying associated with anticyclonic circulation.

347 The influence of cyclonic-like circulation on ozone pollution is spatially heterogeneous, with the  
348 strongest concentration enhancement occurring over the western NCP (with anomalies up to 18.6 ppb),  
349 while impacts over the central and eastern plain remain comparatively weak. This pattern is mainly  
350 attributed to the foehn-induced anomalous warming that promotes photochemical ozone production,  
351 as well as subsidence airflow that transports ozone-rich air from the residual layer downward. As a  
352 result, ozone pollution tends to be most serious along the foothills of the Taihang Mountains in the  
353 western NCP. Further, the prevailing northwesterly winds transport ozone downstream, exerting a  
354 regional influence on ozone pollution across the plain.

355 From a long-term perspective, the frequency of cyclonic-like circulation exhibits an increasing trend,  
356 with 0.24% yr<sup>-1</sup> ( $p < 0.05$ ) from 1980 to 2024, suggesting its growing importance in modulating ozone  
357 pollution. Regional emission reduction experiments show that, under cyclonic-like circulation, local  
358 precursor controls within the NCP are most effective for mitigating ozone pollution, with a 50%  
359 reduction in NO<sub>x</sub> and VOCs leading to an ozone decrease of 5.6 ppb. Under anticyclonic circulation,  
360 emission controls in the southeastern region are more effective in controlling ozone pollution over the  
361 NCP due to the southerly transport. These results reveal the important role of cyclonic-like circulation  
362 in driving ozone pollution over the NCP and highlight the need for developing circulation-dependent  
363 emission control strategies.

364 **Data availability.** The near-surface ozone concentration data are from  
365 <https://datacenter.mee.gov.cn/websjzx/queryIndex.vm>. The MERRA-2 reanalysis data are from  
366 <https://gmao.gsfc.nasa.gov/reanalysis/MERRA-2>.

367 **Author contributions.** XPJ and KL designed the research. WHQ performed the analysis and wrote  
368 the original draft. XPJ reviewed and edited the manuscript. LC, XC, ZYL, and ZJY participated in the  
369 discussion of the results. HL and KL supervised the research project.

370 **Competing interests.** The authors declare no conflict of interest.



371 **Acknowledgements.** This work is supported by the National Natural Science Foundation of China  
372 (grant no. 42293320; 42205114), the National Key Research and Development Program of China  
373 (2022YFE0136100), and the Natural Science Foundation Basic Research Program of Jiangsu Province  
374 (BK20240716; BK20240035).

### 375 **References**

- 376 Chen, G., Ji, X., Chen, J., Xu, L., Hu, B., Lin, Z., Fan, X., Li, M., Hong, Y., Chen, J.: Photochemical  
377 pollution during summertime in a coastal city of Southeast China: Ozone formation and  
378 influencing factors. *Atmos. Res.*, 301, 107270, <https://doi.org/10.1016/j.atmosres.2024.107270>,  
379 2024.
- 380 Chen, R., Lu, R.: Role of large-scale circulation and terrain in causing extreme heat in western North  
381 China. *J. Climate*, 29, 2511-2527, <https://doi.org/10.1175/JCLI-D-15-0254.1>, 2016.
- 382 Dang, R., Liao, H., Fu, Y.: Quantifying the anthropogenic and meteorological influences on  
383 summertime surface ozone in China over 2012–2017. *Sci. Total Environ.*, 754, 142394,  
384 <https://doi.org/10.1016/j.scitotenv.2020.142394>, 2021.
- 385 Dong, Y., Li, J., Guo, J., Jiang, Z., Chu, Y., Chang, L., Yang, Y., Liao, H.: The impact of synoptic  
386 patterns on summertime ozone pollution in the North China Plain. *Sci. Total Environ.*, 735,  
387 139559, <https://doi.org/10.1016/j.scitotenv.2020.139559>, 2020.
- 388 Fleming, Z. L., Doherty, R. M., Von Schneidemesser, E., Malley, C. S., Cooper, O. R., Pinto, J. P.,  
389 Colette, A., Xu, X., Simpson, D., Schultz, M. G., Lefohn, A. S., Hamad, S., Moolla, R., Solberg,  
390 S., Feng, Z.: Tropospheric Ozone Assessment Report: Present-day ozone distribution and trends  
391 relevant to human health. *Elem. Sci. Anth.*, 6, 12, <https://doi.org/10.1525/elementa.273>, 2018.
- 392 Fu, T. M., Zheng, Y., Paulot, F., Mao, J., Yantosca, R. M.: Positive but variable sensitivity of August  
393 surface ozone to large-scale warming in the southeast United States. *Nat. Clim. Change*, 5, 454-  
394 458, <https://doi.org/10.1038/nclimate2567>, 2015.
- 395 Gong, C., Liao, H.: A typical weather pattern for ozone pollution events in North China. *Atmos. Chem.*  
396 *Phys.*, 19, 13725-13740, <https://doi.org/10.5194/acp-19-13725-2019>, 2019.
- 397 Gu, S., Wu, S., Yang, L., Hu, Y., Tian, B., Yu, Y., Ma, N., Ji, P., Zhang, B.: Synoptic Weather Patterns  
398 and Atmospheric Circulation Types of PM<sub>2.5</sub> Pollution Periods in the Beijing-Tianjin-Hebei  
399 Region. *Atmosphere*, 14, 942, <https://doi.org/10.3390/atmos14060942>, 2023.
- 400 Hart, M., De Dear, R., Hyde, R.: A synoptic climatology of tropospheric ozone episodes in Sydney,  
401 Australia. *Int. J. Climatol.*, 26, 1635-1649, <https://doi.org/10.1002/joc.1332>, 2006.
- 402 Hegarty, J., Mao, H., Talbot, R.: Synoptic controls on summertime surface ozone in the northeastern  
403 United States. *J. Geophys. Res.-Atmos.*, 112, D14306, <https://doi.org/10.1029/2006JD008170>,  
404 2007
- 405 Intergovernmental Panel on Climate Change (IPCC): Climate Change 2023: Synthesis Report.  
406 Contribution of Working Groups I, II and III to the Sixth Assessment Report of the  
407 Intergovernmental Panel on Climate Change. <https://doi.org/10.59327/IPCC/AR6-9789291691647>, 2023.
- 409 Jiang, Z., Zhu, B., Shi, S., Yang, S., Tang, G., Lu, W., An, J., Lu, C., Li, K., Liao, H.: Aerosol radiation  
410 effect outweighs VOCs reactivity effect on vertical ozone photochemical features. *J. Geophys.*  
411 *Res.-Atmos.*, 130, e2024JD042348, <https://doi.org/10.1029/2024JD042348>, 2025.
- 412 Kalabokas, P. D., Thouret, V., Cammas, J. P., Volz-Thomas, A., Boulanger, D., Repapis, C. C.: The



- 413 geographical distribution of meteorological parameters associated with high and low summer  
414 ozone levels in the lower troposphere and the boundary layer over the eastern Mediterranean  
415 (Cairo case). *Tellus B*, 67, 27853, <https://doi.org/10.3402/tellusb.v67.27853>, 2015.
- 416 Lamb, H. H.: British Isles weather types and a register of the daily sequence of circulation patterns  
417 1861-1971. *Geophys. Mem.*, 116, <https://ueaeprints.uea.ac.uk/id/eprint/78589>, 1972.
- 418 Lee, Y. C., Shindell, D. T., Faluvegi, G., Wenig, M., Lam, Y. F., Ning, Z., Hao, S., Lai, C. S.: Increase  
419 of ozone concentrations, its temperature sensitivity and the precursor factor in South China. *Tellus*  
420 *B*, 66, 23455, <https://doi.org/10.3402/tellusb.v66.23455>, 2014.
- 421 Lelieveld, J., Crutzen, P. J.: Influences of cloud photochemical processes on tropospheric ozone.  
422 *Nature*, 343, 227-233, <https://doi.org/10.1038/343227a0>, 1990.
- 423 Li, C., Zhu, Q., Jin, X., Cohen, R. C.: Elucidating contributions of anthropogenic volatile organic  
424 compounds and particulate matter to ozone trends over China. *Environ. Sci. Technol.*, 56, 12906-  
425 12916, <https://doi.org/10.1021/acs.est.2c03315>, 2022.
- 426 Li, D., Shindell, D., Ding, D., Lu, X., Zhang, L., Zhang, Y.: Surface ozone impacts on major crop  
427 production in China from 2010 to 2017. *Atmos. Chem. Phys. Discuss.*, 2021, 1-23,  
428 <https://doi.org/10.5194/acp-22-2625-2022>, 2021a.
- 429 Li, K., Jacob, D. J., Liao, H., Qiu, Y., Shen, L., Zhai, S., Bates, K. H., Sulprizio, M. P., Song, S., Lu,  
430 X., Zhang, Q., Zheng, B., Zhang, Y., Zhang, J., Lee, H. C., Kuk, S. K.: Ozone pollution in the  
431 North China Plain spreading into the late-winter haze season. *Proc. Natl. Acad. Sci.*, 118,  
432 e2015797118, <https://doi.org/10.1073/pnas.2015797118>, 2021b.
- 433 Li, M., Huang, X., Yan, D., Lai, S., Zhang, Z., Zhu, L., Lu, Y., Jiang, X., Wang, N., Wang, T., Song,  
434 Y., Ding, A.: Coping with the concurrent heatwaves and ozone extremes in China under a  
435 warming climate. *Sci. Bull.*, 69, 2938-2947, <https://doi.org/10.1016/j.scib.2024.05.034>, 2024.
- 436 Li, X., Sun, J.: Atmospheric circulation patterns conducive to summer extreme temperature,  
437 precipitation, and vapor pressure deficit events over Northeast China. *J. Climate*, 38, 835-853,  
438 <https://doi.org/10.1175/JCLI-D-23-0640.1>, 2025.
- 439 Li, Y., Yu, C., Tao, J., Lu, X., Chen, L.: Analysis of ozone formation sensitivity in Chinese  
440 representative regions using satellite and ground-based data. *Remote Sens.*, 16, 316,  
441 <https://doi.org/10.3390/rs16020316>, 2024.
- 442 Liu, H., Jacob, D. J., Bey, I., Yantosca, R. M.: Constraints from 210Pb and 7Be on wet deposition and  
443 transport in a global three-dimensional chemical tracer model driven by assimilated  
444 meteorological fields. *J. Geophys. Res.-Atmos.*, 106, 12109-12128,  
445 <https://doi.org/10.1029/2000JD900839>, 2001.
- 446 Liu, Y., Geng, G., Cheng, J., Liu, Y., Xiao, Q., Liu, L., Shi, Q., Tong, D., He, K., Zhang, Q.: Drivers  
447 of increasing ozone during the two phases of clean air actions in China 2013–2020. *Environ. Sci.*  
448 *Technol.*, 57, 8954-8964, <https://doi.org/10.1021/acs.est.3c00054>, 2023a.
- 449 Liu, Z., Wang, B., Wang, C., Sun, Y., Zhu, C., Sun, L., Ynag, N., Fan, G., Sun, X., Xia, Z., Pan, G.,  
450 Zhu, C., Gai, Y., Wang, X., Xiao, Y., Yan, G., Xu, C.: Characterization of photochemical losses  
451 of volatile organic compounds and their implications for ozone formation potential and source  
452 apportionment during summer in suburban Jinan, China. *Environ. Res.*, 238, 117158,  
453 <https://doi.org/10.1016/j.envres.2023.117158>, 2023b.
- 454 Lu, X., Hong, J., Zhang, L., Cooper, O. R., Schultz, M. G., Xu, X., Wang, T., Gao, M., Zhao, Y., Zhang,  
455 Y.: Severe surface ozone pollution in China: a global perspective. *Environ. Sci. Technol. Lett.*, 5,  
456 487-494, <https://doi.org/10.1021/acs.estlett.8b00366>, 2018.
- 457 Lu, X., Zhang, L., Chen, Y., Zhou, M., Zheng, B., Li, K., Liu, Y., Lin, J., Fu, T., Zhang, Q.: Exploring  
458 2016–2017 surface ozone pollution over China: source contributions and meteorological



- 459 influences. *Atmos. Chem. Phys.*, 19, 8339-8361, <https://doi.org/10.5194/acp-19-8339-2019>, 2019.
- 460 Long, X., Han, Y., Wang, Q. Y., Li, X. K., Feng, T., Wang, Y. C., Wang, Y., Zhang, S. L., Han, Y. M.,  
461 Li, G. H., Tie, X. X., Cao, J. J., Chen, Y.: Adverse effects of ozone pollution on net primary  
462 productivity in the North China Plain. *Geophys. Res. Lett.*, 51, e2023GL105209,  
463 <https://doi.org/10.1029/2023GL105209>, 2024.
- 464 Matějka, M., Řehoř, J., Brázdil, R., Štěpánek, P., Zahradníček, P.: Foehn warming mechanism and  
465 near-surface weather impact at the northern foreland of the Moravian-Silesian Beskids, Czech  
466 Republic. *Theor. Appl. Climatol.*, 156, 145, <https://doi.org/10.1007/s00704-024-05337-3>, 2025.
- 467 McLinden, C. A., Olsen, S. C., Hannegan, B., Wild, O., Prather, M. J., Sundet, J.: Stratospheric ozone  
468 in 3-D models: A simple chemistry and the cross-tropopause flux. *J. Geophys. Res.-Atmos.*, 105,  
469 14653-14665, <https://doi.org/10.1029/2000JD900124>, 2000.
- 470 MEE: China's Ecological Environment Situation Bulletin in 2022 (in Chinese). Ministry of Ecology  
471 and Environment of the People's Republic of China,  
472 <https://www.mee.gov.cn/hjzl/sthjzk/zghjzkgb/202305/P020230529570623593284.pdf> (last  
473 access: 15 Sep 2024), 2023.
- 474 MEE: Ministry of Ecology and Environment Announces National Ambient Air Quality Conditions for  
475 June and January-June 2024,  
476 [https://www.mee.gov.cn/ywdt/xwfb/202407/t20240729\\_1082850.shtml](https://www.mee.gov.cn/ywdt/xwfb/202407/t20240729_1082850.shtml) (last access: 11 Mar  
477 2025), 2024.
- 478 Nuvolone, D., Petri, D., Voller, F.: The effects of ozone on human health. *Environ. Sci. Pollut. Res.*,  
479 25, 8074-8088, <https://doi.org/10.1007/s11356-017-9239-3>, 2018.
- 480 Pope, R. J., Butt, E. W., Chipperfield, M. P., Doherty, R. M., Fenech, S., Schmidt, A., Arnold, S. R.,  
481 Savage, N. H.: The impact of synoptic weather on UK surface ozone and implications for  
482 premature mortality. *Environ. Res. Lett.*, 11, 124004, <https://doi.org/10.1088/1748-9326/11/12/124004>, 2016.
- 484 Qu, K., Yan, Y., Wang, X., Jin, X., Vrekoussis, M., Kanakidou, M., Brasseur, G. P., Lin, T., Xiao, T.,  
485 Cai, X., Zeng, L., Zhang, Y.: The effect of cross-regional transport on ozone and particulate matter  
486 pollution in China: A review of methodology and current knowledge. *Sci. Total Environ.*, 947,  
487 174196, <https://doi.org/10.1016/j.scitotenv.2024.174196>, 2024.
- 488 Tarvainen, V., Hakola, H., Hellén, H., Bäck, J., Hari, P., Kulmala, M.: Temperature and light  
489 dependence of the VOC emissions of Scots pine. *Atmos. Chem. Phys.*, 5, 989-998,  
490 <https://doi.org/10.5194/acp-5-989-2005>, 2005.
- 491 Wang, T., Xue, L., Feng, Z., Dai, J., Zhang, Y., Tan, Y.: Ground-level ozone pollution in China: a  
492 synthesis of recent findings on influencing factors and impacts. *Environ. Res. Lett.*, 17, 063003,  
493 <https://doi.org/10.1088/1748-9326/ac69fe>, 2022.
- 494 Wang, Z. B., Li, J. X., Liang, L. W.: Spatio-temporal evolution of ozone pollution and its influencing  
495 factors in the Beijing-Tianjin-Hebei Urban Agglomeration. *Environ. Pollut.*, 256, 113419,  
496 <https://doi.org/10.1016/j.envpol.2019.113419>, 2020.
- 497 Wang, Z., Zhang, H., Shi, C., Ji, X., Zhu, Y., Xia, C., Sun, X., Zhang, M., Lin, X., Yan, S., Zhou, Y.,  
498 Xing, C., Chen, Y., Liu, C.: Vertical and spatial differences in ozone formation sensitivities under  
499 different ozone pollution levels in eastern Chinese cities. *npj Clim. Atmos. Sci.*, 8, 30,  
500 <https://doi.org/10.1038/s41612-024-00855-3>, 2025.
- 501 Weng, H., Lin, J., Martin, R., Millet, D. B., Jaeglé, L., Ridley, D., Keller, C., Li, C., Du, M., Meng, J.:  
502 Global high-resolution emissions of soil NO<sub>x</sub>, sea salt aerosols, and biogenic volatile organic  
503 compounds. *Sci. Data*, 7, 148, <https://doi.org/10.1038/s41597-020-0488-5>, 2020.
- 504 Wesely, M. L.: Parameterization of surface resistances to gaseous dry deposition in regional-scale



- 505 numerical models. *Atmos. Environ.*, 41, 52-63, <https://doi.org/10.1016/j.atmosenv.2007.10.058>,  
506 2007.
- 507 Xie, Q., Tham, Y. J., Yu, X., Wang, Z., Ling, Z., Wang, X., Guo, H., Wang, T.: Seasonal variations of  
508 O<sub>3</sub> formation mechanism and atmospheric photochemical reactivity during severe high O<sub>3</sub>  
509 pollution episodes in the Pearl River Delta region. *Atmos. Environ.*, 309, 119918,  
510 <https://doi.org/10.1016/j.atmosenv.2023.119918>, 2023.
- 511 Xing, J., Ning, G., Zhang, X., Zhu, B., Cheng, M., Zhao, T., Wang, J., Yang, Y.: Persisting day and  
512 night high surface ozone pollution driven by compound heatwaves. *Geophys. Res. Lett.*, 53,  
513 e2025GL121138, <https://doi.org/10.1029/2025GL121138>, 2026.
- 514 Xu, T., Gao, X., Jiang, S., Hu, K., Peng, Z., Zhao, X., Tang, X.: Nonlinear ozone response to extreme  
515 high temperature in a subtropical megacity basin: Integrated observation and modeling analysis.  
516 *Environ. Res.*, 285, 122274, <https://doi.org/10.1016/j.envres.2025.122274>, 2025.
- 517 Xue, L., Zhu, Y., Gao, J., Zhong, X., Cui, C., Wang, S., Jiang, Z., Sun, Y., Li, Q., Zhang, Y., Li, H.,  
518 Zhang, Y., Wang, S., Zhao, M., Shen, H., Zhang, Y., Tang, G., Wang, T., Wang, W.: Critical  
519 transition of urban ozone formation regime in the North China Plain. *Natl. Sci. Rev.*, 13, nwaf596,  
520 <https://doi.org/10.1093/nsr/nwaf596>, 2026.
- 521 Yan, F., Su, H., Cheng, Y., Huang, R., Liao, H., Yang, T., Zhu, Y., Zhang, S., Sheng, L., Kou, W., Zeng,  
522 X., Xiang, S., Yao, X., Gao, H., Gao, Y.: Frequent haze events associated with transport and  
523 stagnation over the corridor between the North China Plain and Yangtze River Delta. *Atmos.*  
524 *Chem. Phys.*, 24, 2365-2376, <https://doi.org/10.5194/acp-24-2365-2024>, 2024.
- 525 Zhang, X., Han, D., Shen, J., Chen, F., Cao, L., Chen, J., Lin, X., Yang, Y., Yang, L., Li, W., Qiao, X.,  
526 Zhou, S., Zhang, Q., Shi, J., Jiang, G.: Unraveling ozone formation sensitivity to ambient VOCs  
527 and NO<sub>x</sub> at urban and mountain sites in a typical city of eastern China. *Environ. Pollut.*, 385,  
528 127063, <https://doi.org/10.1016/j.envpol.2025.127063>, 2025.